Pis'ma v ZhETF, vol. 107, iss. 2, pp. 119 – 120 © 2018 January 25

Topology of the ^{3}He-A film on corrugated graphene substrate

G. E. Volovik[1)]

Low Temperature Laboratory, Aalto University, P.O. Box 15100, FI-00076 Aalto, Finland

Landau Institute for Theoretical Physics, 142432 Chernogolovka, Russia

P.N. Lebedev Physical Institute, RAS, 119991 Moscow, Russia

Submitted 29 November 2017

DOI: 10.7868/S0370274X18020091

Graphene and topological phases of superfluid ^{3}He have many common properties. In both systems quasiparticles behave as relativistic fermions, being protected by symmetry and topology. These two systems can be combined to produce new phenomena [1]. Using the thin film of the chiral superfluid ^{3}He-A and time reversal invariant planar phase deposited on graphene substrate, one may study the effect of disorder in $2+1$ topological systems, which experience the intrinsic quantum Hall and intrinsic spin quantum Hall effects respectively [2, 3]. On one hand graphene can be made atomically smooth, which is the necessary condition for the superfluidity in thin films of ^{3}He. On the other hand it is corrugated, providing disorder for ^{3}He film.

On a flat graphene sheet, the film is characterized by the integer valued topological invariant (Chern number) in terms of Green's function $\mathcal{G}(p_x, p_y, \omega)$:

$$\tilde{N}_3 = \frac{1}{4\pi^2}\mathbf{tr}\left[\int d^2p d\omega\ \mathcal{G}\partial_{p_x}\mathcal{G}^{-1}\mathcal{G}\partial_{p_y}\mathcal{G}^{-1}\mathcal{G}\partial_{\omega}\mathcal{G}^{-1}\right]. \quad (1)$$

This topological charge determines the quantized Hall conductance in charged ^{3}He-A [4, 2]:

$$\sigma_{xy} = \frac{1}{2}\frac{e^2}{h}\tilde{N}_3. \quad (2)$$

Because of the Majorana nature of Bogoliubov quasiparticles, it is twice smaller than $\sigma_{xy} = \tilde{N}_3(e^2/h)$ in the non-superconducting systems [5–7] $\tilde{N}_3$ also determines the number of topological edge states [8].

In the ^{3}He film, $\tilde{N}_3$ depends on the film thickness a. For atomically thin films, $\tilde{N}_3$ is proportional to the number of atomic layers. With increasing of the thickness towards the bulk limit the Weyl points in the spectrum are formed. In this $3+1$ limit, at each value of the momentum k_z the system represents the $2+1$ superfluid. In the interval $|k_z| < k_{\rm F}$ between the Weyl nodes these superfluids are topolically nontrivial with the charge $\tilde{N}_3 = 2$. As a result the total Chern number of the thick film is determined by the splitting $2k_{\rm F}$ of the Weyl nodes: $\tilde{N}_3 = 2(2k_{\rm F}a/2\pi)$, see also [9]. In this limit, the topological edge states form the flat band with zero energy in the whole interval $-k_{\rm F} < k_z < k_{\rm F}$ [10, 11].

For ^{3}He-A on corrugated graphene, the thickness of the film $a(x, y)$ depends on the coordinates. If the corrugation is smooth, one can introduce the local topological charge $\tilde{N}_3(x, y)$, using the local Green's function $G(\mathbf{p}, \mathbf{r}, \omega)$, where $\mathbf{r} = (\mathbf{r}_2 + \mathbf{r}_1)/2$ is the center of mass coordinate. Fig. 1 illustrates the spatial distribution of

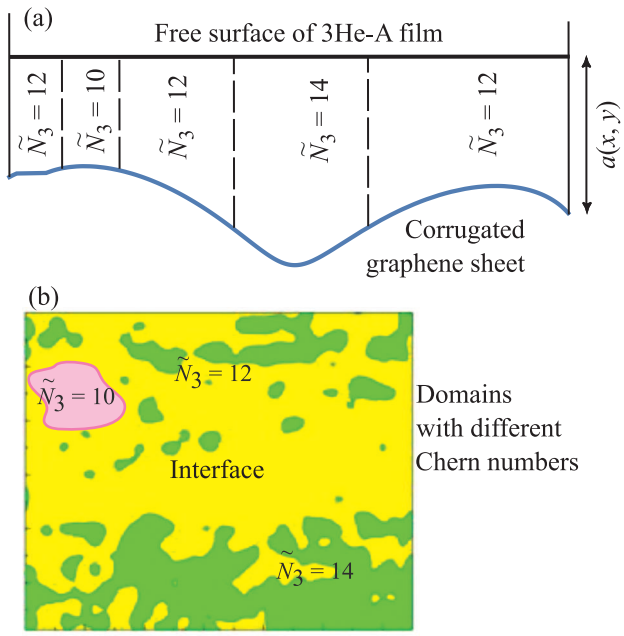

Fig. 1. (Color online) Illustration of the distribution of the values of topological invariant in the ^{3}He-A film on the corrugated graphene. The local topological invariant $\tilde{N}_3(x, y)$ in Eq. (1) can be constructed using the local Green's function $G(\mathbf{p}, \mathbf{r}, \omega)$. (a) – The system can be represented as collection of domains with different $\tilde{N}_3$ – the space analog of the Chern mosaic [12, 13]. σ_{xy} is determined by $\tilde{N}_3$ of the percolated domain. The domains with other values of $\tilde{N}_3$ are the finite islands. (b) – This picture illustrates the configuration with the two infinite domains, with $\tilde{N}_3 = 12$ and $\tilde{N}_3 = 14$, which are separated by the infinite interface with fermion zero mode

[1)]e-mail: volovik@boojum.hut.fi

the local Chern number $\tilde{N}_3(x, y)$. Regions with the same value of invariant form either closed islands or the percolating cluster. Domains with different $\tilde{N}_3$ are separated by lines, which contain the edge states. In case of a single percolated domain, its charge $\tilde{N}_3$ determines the value of σ_{xy} of the whole sample. The current is formed by delocalized states on boundaries of graphene.

The boundaries of the finite islands also contain the edge states, but these states are localized in the island. The boundary of the dominating domain has infinite length and contains exact zero modes, whose number $\tilde{N}_3$ determines the integer valued conductance. The state of the film may contain two percolated domains, see Fig. 1. They are separated by the infinite interface with exact zero modes, whose algebraic number equals $\tilde{N}_3^{(2)} - \tilde{N}_3^{(1)}$, due to counterpropagating modes.

On semiclassical level, domain boundaries contain lines of zeroes of the inverse Green's function $G^{-1}(\mathbf{p}, \mathbf{r}, \omega)$ in the 5-dimensional (p_x, p_y, x, y, ω)-space. These nodal lines are described by the topological charge N_3, where the integral is over the S^3 spheres around the line. According to the Atiyah–Bott–Shapiro construction [14], the effective Hamiltonian in the vicinity of the line is $H = \sigma_x c_x p_x + \sigma_y c_y p_y + q\sigma_z x$, where the coordinate y is locally along the line, and the variables (x, p_x, p_y) are perpendicular to the line. On the quantum level, one has Majorana modes, whose spectrum $E = \tilde{c}_y p_y$ crosses zero as a function of p_y [15]. In the islands, the energy of the edge states is on the order of $|E| \sim c_y/L$, where L is the length of the boundary of the island. The distribution of islands determines statistical properties of the low-energy states of the system. All this can be applied to electronic systems, see, e.g. [16].

In conclusion, we considered the $2 + 1$ topological system with a smooth type of disorder, which can be considered as a Chern mosaic – a collection of domains with different topological Chern numbers. The quantization of the Hall conductance is determined by the macroscopic percolated domain, while the density of the fermionic states in bulk [17] is determined by the edge modes of finite domains. This system can be useful for the general consideration of disorder in the topological matter [18–23].

The bulk 3D topological system with smooth disorder has been realized in ^{3}He-A in aerogel [24, 25]. This is a superfluid realization of the skyrmion glass suggested for magnets [26]. In the ^{3}He-A case, skyrmions are 3-dimensional [27], described by the Hopf invariant in terms of helicity [28–30]. The Weyl nodes are smoothly distributed in space forming a Weyl glass. The effective tetrad field experienced by the Weyl fermions is the analog of "torsion foam" [31, 32] with $\langle e_a^\mu \rangle = 0$.

I acknowledge support by RSF (# 16-42-01100).

Full text of the paper is published in JETP Letters journal. DOI: 10.1134/S0021364018020054

1. M. I. Katsnelson and G. E. Volovik, J. Low Temp. Phys. **175**, 655 (2014).
2. G. E. Volovik, *Exotic Properties of Superfluid ^{3}He*, World Scientific (1992).
3. Yu. Makhlin, M. Silaev, and G.E. Volovik, Phys. Rev. B **89** 174502 (2014).
4. G. E. Volovik, JETP **67**, 1804 (1988).
5. H. So, Prog. Theor. Phys. **74**, 585 (1985).
6. K. Ishikawa and T. Matsuyama, Z. Phys. C **33**, 41 (1986).
7. K. Ishikawa and T. Matsuyama, Nucl. Phys. B **280**, 523 (1987).
8. G. E. Volovik, JETP lett. **55**, 368 (1992).
9. A. A. Burkov, Phys. Rev. Lett. **120**, 016603 (2018).
10. N. B. Kopnin and M. M. Salomaa, Phys. Rev. B **44**, 9667 (1991).
11. G. E. Volovik, JETP Lett. **93**, 66 (2011)
12. J. Röntynen and T. Ojanen, Phys. Rev. B **93**, 094521 (2016).
13. K. Pöyhönen and T. Ojanen, Phys. Rev. B **96**, 174521 (2017).
14. P. Hořava, Phys. Rev. Lett. **95**, 016405 (2005).
15. G. E. Volovik, *The Universe in a Helium Droplet*, Clarendon Press, Oxford (2003)
16. E. M. Chudnovsky, Phys. Rev. B **33**, 245 (1986).
17. R. Movassagh, Phys. Rev. Lett. **119**, 220504 (2017).
18. T. Morimoto, A. Furusaki, and Ch. Mudry, Phys. Rev. B **91**, 235111 (2015).
19. J. Song and E. Prodan, Phys. Rev. B **92**, 195119 (2015).
20. R.-J. Slager, L. Rademaker, J. Zaanen, and L. Balents, Phys. Rev. B **92**, 085126 (2015).
21. E. Prodan, arXiv:1602.00306.
22. B. Lian, J. Wang, X.-Q. Sun, A. Vaezi, and Sh.-Ch. Zhang, arXiv:1709.05558.
23. B. Wu, J. Song, J. Zhou, and H. Jiang, Chin. Phys. B **25**, 117311 (2016).
24. G. E. Volovik, J. Low Temp. Phys. **150**, 453 (2008).
25. V. V. Dmitriev, D. A. Krasnikhin, N. Mulders, A. A. Senin, G. E. Volovik, and A. N. Yudin, JETP Lett. **91**, 599 (2010).
26. E. M. Chudnovsky and D. A. Garanin, arXiv:1710.10608.
27. T. H. R. Skyrme, Nucl. Phys. **31**, 556 (1962).
28. G. E. Volovik and V. P. Mineev, JETP **46**, 401 (1977).
29. V. M. H. Ruutu, Ü. Parts, J. H. Koivuniemi, M. Krusius, E. V. Thuneberg, and G. E. Volovik, JETP Lett. **60**, 671 (1994).
30. Yu. G. Makhlin and T. Sh. Misirpashaev, JETP Lett. **61**, 49 (1995).
31. S. W. Hawking, Nucl. Phys. B **144**, 349 (1978).
32. A. J. Hanson and T. Regge, Lect. Notes Phys. **94**, 354 (1979).